EUROPEAN RESPIRATORY *journal*

FLAGSHIP SCIENTIFIC JOURNAL OF ERS

Early View

Original article

Effective control of *S. aureus* lung infection despite tertiary lymphoid structures disorganisation

Lucile Regard, Clémence Martin, Jean-Luc Teillaud, Hélène Lafoeste, Hugues Vicaire, Maha Zohra Ladjemi, Emilie Ollame-Omvane, Sophie Sibéril, Pierre-Régis Burgel

Please cite this article as: Regard L, Martin Cémence, Teillaud J-L, *et al*. Effective control of *S. aureus* lung infection despite tertiary lymphoid structures disorganisation. *Eur Respir J* 2020; in press (https://doi.org/10.1183/13993003.00768-2020).

Title: Effective control of *S. aureus* lung infection despite tertiary lymphoid structures disorganization

Running Title: Tertiary lymphoid structures in *S. aureus* lung infection

Authors: Lucile Regard[1,2], Clémence Martin[1,2], Jean-Luc Teillaud[3,4], Hélène Lafoeste[1,2], Hugues Vicaire[1,2], Maha Zohra Ladjemi[1], Emilie Ollame-Omvane[5], Sophie Sibéril[5]*, Pierre-Régis Burgel[1,2*]

* These authors equally contributed to this work.

Affiliations:

[1] Institut Cochin and Université de Paris, INSERM U1016, Paris, France

[2] Service de Pneumologie, Hôpital Cochin, AP-HP, Paris, France.

[3] Laboratory "Immune microenvironment and immunotherapy", Centre d'Immunologie et des Maladies Infectieuses (CIMI), Paris, France

[4] INSERM UMRS 1135, Faculté de Médecine, Sorbonne Université, Paris, France

[5] Centre de Recherche des Cordeliers, INSERM, Sorbonne Université, Université de Paris, F-75006 Paris, France

Corresponding author: Pierre-Régis Burgel MD, PhD

27, rue du Faubourg Saint Jacques

75014 Paris, France.

Tel: + 33 1 58 41 23 67

Fax: +33 1 46 33 82 53

E-mail: pierre-regis.burgel@aphp.fr

Take home message (max: 256 signs): 249 signs.

Disorganization of peribronchial lymphoid follicles did not result in increased bacterial load nor in decreased survival in a mouse model of persistent lung infection. Lymphoid follicles may not be essential for controlling lung bacterial infection.

Abstract: 232 words (250 max)

Background: Tertiary lymphoid structures (TLS) are triggered by persistent bronchopulmonary infection with *S. aureus* but their roles remain elusive. The present study sought to examine the effects of B and/or T cell depletion on *S. aureus* infection and TLS development (lymphoid neogenesis) in mice.

Methods: C57Bl/6 mice were pretreated with (1) an anti-CD20 mAb (B cell depletion) or (2) an anti-CD4 and/or an anti-CD8 mAbs (T cell depletion) or (3) a combination of anti-CD20, anti-CD4 and anti-CD8 mAbs (combined B and T cell depletion) or (4) with isotype control mAbs. After lymphocyte depletion, mice were infected by intratracheal instillation of agarose beads containing *S. aureus* (10^6 CFU/mouse). Fourteen days later, bacterial load and lung inflammatory cell infiltration were assessed by cultures and immunohistochemistry, respectively.

Results: Fourteen days after *S. aureus*-bead instillation, lung bacterial load was comparable between control and lymphocyte-depleted mice. While TLS were observed in the lungs of infected mice pretreated with control mAbs, these structures were disorganized or abolished in the lungs of lymphocyte-depleted mice. The absence of $CD20^+$ B lymphocytes had no effect on $CD3^+$ T lymphocyte infiltration, whereas $CD4^+$/$CD8^+$ T-cell depletion markedly reduced $CD20^+$ B cell infiltration. Depletion of $CD4^+$ or $CD8^+$ T cells separately had limited effect on B cell infiltration but lead to the absence of germinal center.

Conclusion: TLS disorganization is not associated with loss of infection control in mice persistently infected with *S. aureus*.

Word count: 3133

Introduction

Immune response in the airways of patients with cystic fibrosis (CF) or non-CF bronchiectasis diseases is dominated by increased innate immunity with airway mucus plugging (1, 2) and massive neutrophilic infiltration (3-5). However, studies using lung explants obtained in CF patients (6-9) or using surgically resected lung tissues in patients with bronchiectasis (6, 10) have found evidence of intrapulmonary adaptive immune response, characterized by the presence of peribronchial aggregates of B and T lymphocytes. These lymphoid aggregates were often organized into tertiary lymphoid structures (TLS) containing segregated B and T cell areas, high endothelial venules (HEVs), follicular dendritic cells (FDCs) and germinal centers (6). Persistent airway infection of C57/Bl6 mice with *P. aeruginosa* or with *S. aureus*, two major bacteria found in the airways of patients with CF, triggered the development of peribronchial TLS (a process called lymphoid neogenesis) within 14 days (6, 11). These data suggest that TLS found in patients with CF or non-CF bronchiectasis contribute to the immune response triggered by chronic bacterial infection (6).

Mechanisms leading to lymphoid neogenesis in the lungs have been partly elucidated (12), but roles of TLS in chronic airway diseases associated with bacterial infection remain elusive. TLS may contribute to the immune response against bacterial infection (13, 14), limiting the extent of airway infection *via* the production of antibodies by activated B cells. Alternatively bacterial infection could induce lung tissue damage, which might result in the release of self-antigens, giving rise to B and T cell responses that perpetuate tissue injury (13, 14). Thus, it remains unclear whether targeting lung lymphoid neogenesis would be detrimental or beneficial in airway diseases associated with chronic bacterial infection.

In the present study, we analyzed the roles of adaptive immune components of TLS in chronic lung infection by selectively blocking recruitment of lymphocyte subsets using monoclonal antibodies (mAbs) in a mouse model of persistent *S. aureus* infection. Thus, we targeted B and/or $CD4^+$ and $CD8^+$ T

lymphocytes before inducing persistent *S. aureus* infection and explored the effects on bacterial infection and lung lymphoid neogenesis.

Methods

Murine model of persistent airway infection

Female C57Bl/6 mice (aged 6 to 8 weeks) were purchased from Janvier (Saint Berthevin, France). Persistent airway infection was obtained by intratracheal instillation of agarose beads containing *S. aureus* (10^6 CFU per animal) as described previously (6), and euthanized 14 days after instillation. All animal experiments received approval (#4664 and #12190) from the ethical review board Charles Darwin (Sorbonne University).

Depletion of $CD20^+$ B cells and/or $CD4^+$/$CD8^+$ T cells

Depletion of $CD20^+$ B cells and/or $CD4^+$/$CD8^+$ T cells was obtained by injection of anti-CD20 and/or anti-CD4 and anti-CD8 depleting mAbs, respectively, as described in **Figure 1**. For $CD20^+$ B cell depletion, one dose of 250µg of mouse IgG2a anti-mouse CD20 mAb (clone 5D2, kindly provided by Genentech, San Francisco, CA, USA) was injected intravenously (*i.v.*) 7 days before *S. aureus*-containing beads instillation (**Figure 1A**). For $CD4^+$ and $CD8^+$ T-cell depletion experiments, mice received intraperitoneal (*i.p.*) injections of 250µg anti-mouse CD4 mAb (rat IgG2b, clone GK1.5; BioXCell, West Lebanon, NH, USA), and 250µg anti-mouse CD8 mAb (rat IgG2b, clone YTS169.4; BioXCell), respectively 5 and 4 days before *S. aureus*-containing beads instillation. Mice received a second *i.p.* injection of 250µg anti-CD4 and 250 µg anti-CD8 mAbs 4 and 5 days after intratracheal instillation, respectively (**Figure 1B**). One group of mice received anti-CD20 mAb combined to anti-CD4 and anti-CD8 mAbs (combined B and $CD4^+$/$CD8^+$ T cell depletion, **Figure 1C**).

To further explore the respective roles of $CD4^+$ or $CD8^+$ T cells in the development of TLS, two groups of mice were depleted of either $CD4^+$ or $CD8^+$ T cells by two *i.p.* injections of 250µg rat anti-mouse CD4 or 250µg rat anti-mouse CD8, respectively.

Control groups of mice received similar doses of isotype-matched control mAbs (mouse IgG2a mAb, clone C1.18.4 and/or rat IgG2b mAb, clone LTF-2; BioXCell). Depletion of $CD20^+$ B cells and/or $CD4^+$/$CD8^+$ T cells was confirmed by flow cytometry analysis of the blood of animals, one day before *S. aureus*-bead instillation. Only animals exhibiting blood percentages of B cells and/or CD4 and CD8 T cells below 5% after pretreatment with mAbs were subsequently infected with *S. aureus*-containing beads.

Lung bacterial load

Mice were euthanized 14 days after *S. aureus*-containing beads instillation and 10-fold dilutions of total lung homogenates were plated on trypticase soy agar. CFU count was performed after 24-hour incubation at 37°C.

Immunohistochemical staining

Lungs were removed after flushing 4% paraformaldehyde through the right heart and insufflated 5 minutes with 4% paraformaldehyde at -20cm H_20. Five-µm paraffin sections of mouse lungs were immunostained as described previously (6) for detecting B lymphocytes ($CD20^+$), T lymphocytes ($CD3^+$), HEVs (peripheral node adressin ($PNAd^+$)), FDCs ($CD21^+$) and proliferating cell nuclear antigen ($PCNA^+$; for the identification of germinal centers). A detailed description of the sources of primary antibodies, dilutions and unmasking techniques is provided in **supplementary Table S1**. Biotinylated anti-mouse, anti-rabbit, anti-rat or anti-goat antibodies (dilution 1:200; Vector Laboratories, Burlingame, CA, USA) were used for secondary antibodies and bound antibodies were visualized according to standard

protocols for avidin–biotin–peroxidase complex method (Elite ABC kit; Vector Laboratories). Tissue sections were counterstained with hematoxylin (Vector Laboratories).

Morphometric analyses

Quantitative morphometric analysis was performed by two independent observers using a light microscope (Leica Microsystems, Wetzlar, Germany) connected to a computer (6). A lymphoid aggregate was defined as a $CD20^+$ or $CD3^+$ cell aggregate that could be detected using a low-power field (X16). Briefly, images were collected using a light microscope connected to the Leica Application Suite software (v 4.1.0, Leica Microsystems) and the outline tool in Image J software (v 1.48, National Institute of Health, USA) was used for measuring tissue area. The number of lymphoid aggregates was expressed per cm^2 of lung tissue.

Flow cytometry

Surface staining of blood and lung cells was performed according to standard protocols and analyzed using a LSRFortessa (BD Biosciences) flow cytometer and Kaluza software (Beckman Coulter). For flow cytometry analyses of pulmonary tissue, lungs were flushed with phosphate buffered saline (PBS) through the right heart, harvested and immediately stored at 4°C in staining buffer (PBS, BSA 0.5% and EDTA 2mM). Lungs were then incubated for one hour at 37°C in RPMI medium supplemented with, 200µg/ml Liberase TL, 0.1 mg/ml DNAse I (Roche Diagnostics GmbH, Mannheim, Germany) and 0.5mM EDTA. Red blood cells were eliminated using ACK (Ammonium Chloride Potassium) lysis buffer. Blood and lungs cells were stained with antibodies as described in **supplementary Table S2**.

Statistical analysis

Data obtained from morphometric and flow cytometry analyses were analyzed using the nonparametric Mann-Whitney or Kruskal-Wallis tests. The interobserver coefficients of variation for morphometric

measurements were always <15%. All analyses were performed using Prism 8 software (GraphPad, La Jolla, CA, USA). *P* values < 0.05 were considered statistically significant.

Results

Effects of CD20$^+$ B lymphocyte and/or CD4$^+$/CD8$^+$ T lymphocyte depletion on S. aureus lung infection

We first established protocols to obtain depletion of CD20$^+$ B cells and/or CD4$^+$/CD8$^+$ T cells that persisted all along the 14 days of *S. aureus* infection in C57Bl/6 mice. A single *i.v.* injection of anti-CD20 mAb induced B cell depletion in the lungs, which persisted for at least 21 days as confirmed by flow cytometry and immunohistochemical staining (**supplementary Figure S1**). Injections of anti-CD4 and anti-CD8 mAbs repeated every 9 days also induced persistent CD4$^+$/CD8$^+$ T cell depletion in the lungs (**supplementary Figure S1**). Injection of control mAbs had no effect on CD20$^+$ B cells and CD4$^+$/CD8$^+$ cells in the lungs.

To study the effect of CD20$^+$ B cell and/or CD4$^+$/CD8$^+$ T cell depletion on *S. aureus* infection, C57Bl/6 mice were injected with anti-CD20 and/or anti-CD4/CD8 mAbs prior to intratracheal instillation of agarose beads containing *S. aureus* (10^6 CFU/animal); animals were euthanized at 14 days after infection (**Figure 1**). In all experimental groups, none of the mice died during the 14 days of infection. Treatment with anti-CD20 and/or anti-CD4/CD8 mAbs had no significant effect on lung bacterial load at 14 days after intratracheal instillation (**supplementary Figure S2**).

Effects of CD20$^+$ B lymphocyte depletion and/or CD4$^+$/CD8$^+$ T lymphocyte depletion on S. aureus-induced peribronchial lymphoid neogenesis

As described previously, *S. aureus* infection resulted in peribronchial lymphoid neogenesis within 14 days (6), a process that was not affected by pretreatment with control mAbs. Fourteen days after instillation of *S. aureus*-containing beads, peribronchial lymphoid aggregates were found around bead-

containing bronchi; these aggregates contained B-cell areas ($CD20^+$) with follicular dendritic cells ($CD21^+$) and germinal centers ($PCNA^+$) and were surrounded by T cell aggregates ($CD3^+$) containing high endothelial venules ($PNAd^+$) and were consistent with tertiary lymphoid structures. Representative photomicrographs can be found in **supplementary Figure S3**.

Pretreatment with anti-CD20 mAb prior to *S. aureus* infection was marked by an absence of peribronchial B cells, $CD21^+$ FDCs (**Figure 2** and **Figure 3A**) and germinal centers (**supplementary Figures S4 and S5)**. By contrast, $CD3^+$ T-cell recruitment (**Figure 2** and **Figure 3A**) and HEV formation were unaffected (**supplementary Figures S4 and S5)**.

Pretreatment with anti-CD4/CD8 mAbs prior to *S. aureus* infection markedly reduced the presence of $CD3^+$ T cells, although small peribronchial $CD3^+$ (presumably $CD4^-/CD8^-$) T cell aggregates were found around bead-containing airways (**Figure 2**). Treatment with anti-CD4/CD8 mAbs also reduced HEV formation and abolished germinal center formation (**supplementary Figures S4 and S5)**. Surprisingly, treatment with anti-CD4/CD8 mAbs reduced the presence of peribronchial $CD20^+$ B lymphocytes and $CD21^+$ FDC (**Figure 2** and **Figure 3B**). Treatment with anti-CD4/CD8 mAbs significantly reduced both the number (**Figure 4A**) and size (**Figure 4F**) of *S. aureus*-induced $CD20^+$ lymphoid aggregates by approximatively 3 and 6 times, respectively. To further explore respective roles of $CD4^+$ and $CD8^+$ T cells in *S. aureus*-induced TLS formation, two groups of mice were pretreated either with anti-CD4 or anti-CD8 mAbs prior to *S. aureus* infection. Pretreatment with anti-CD4 or anti-CD8 mAbs did not reduce the number of $CD20^+$ (**Figure 4A**) or CD3+ (**Figure 4D**) peribronchial lymphoid aggregates, the recruitment of FDCs (**Figure 4B**) and the number of HEVs (**Figure 4E**) but prevented germinal center formation (**Figure 4C**). However, injection of anti-CD4 mAb reduced the size of $CD20^+$ peribronchial lymphoid aggregates (**Figure 4F**).

Finally, pretreatment with anti-CD20 and anti-CD4/CD8 mAbs prior to *S. aureus* infection completely prevented lymphoid neogenesis. As expected, peribronchial B cell presence as well as $CD21^+$ FDC recruitment and germinal center formation were abolished. Peribronchial $CD3^+$ T cell recruitment and HEV formation were also markedly reduced (**Figure 2**, **Figure 3C, supplementary Figures S4 and S5**).

Discussion

In the present study, we examined the roles of $CD20^+$ B lymphocytes and/or $CD4^+$/$CD8^+$ T lymphocytes in antibacterial response and peribronchial lymphoid neogenesis in a mouse model of persistent *S. aureus* lung infection. Our results indicated that (A) blockade of lymphoid neogenesis was not associated with increased mortality or increased lung bacterial load in mice infected with *S. aureus* for 14 days; (B) $CD20^+$ B lymphocytes, $CD4^+$ and $CD8^+$ T lymphocytes were all required for lymphoid neogenesis and germinal center formation; (C) the absence of $CD20^+$ B lymphocytes had no effect on the development of $CD3^+$ T cell peribronchial aggregates, whereas $CD4^+$/$CD8^+$ T cell depletion markedly reduced $CD20^+$ B cell aggregates. These findings provide further insights on mechanisms of bacteria-driven lymphoid neogenesis in the lungs and possible roles of TLS in chronic airway diseases.

Because lymphoid follicles harboring characteristics of TLS developed as a consequence of persistent bacterial infection in mouse airways (6), we hypothesized that these TLS contributed to the control of lung infection. This hypothesis was reinforced by recent findings from Ladjemi et al. who reported an increased IgA production by TLS during persistent *P. aeruginosa* infection in mice and found that bronchoalveolar lavage IgA were directed toward *P. aeruginosa* (15). However, disorganization of lymphoid neogenesis using anti-CD20 and/or anti-CD4/CD8 mAbs did not result in reduced infection control as we found no evidence of increased bacterial load and no evidence of decreased survival in these experiments. To the best of our knowledge, no other study examined possible roles of TLS in the control of chronic airway bacterial infection. Previous studies have yielded somewhat different results on the possible anti-infective roles of TLS in the lungs (13). Moyron-Quiroz et al. first suggested that lung lymphoid follicles with characteristics of TLS contributed to infection control in mice lacking secondary lymphoid organs infected by influenza virus (16), presumably through maturation and selection of B cells directed against influenza virus nucleoprotein (17). Studies in mice lacking IL-23 or CXCR5 have also

demonstrated that disorganized lung TLS are associated with poor protective immune response against *M. tuberculosis* (18, 19), suggesting a role for TLS in *M. tuberculosis* containment. Eddens et al. showed that *Pneumocystis* infection induced TLS containing germinal centers in the lung (20); studies in lymphotoxin-α (LTα) deficient mice resulted in smaller, disorganized, lymphoid follicles lacking germinal centers, with lower numbers of proliferating B cells. However, LTα deficient mice were able to clear *Pneumocystis* at day 14 post infection like wild-type C57Bl/6 mice (20), indicating that TLS were not required for *Pneumocystis* clearance. We suggest that bacteria-driven TLS may contribute to immune response (e.g., via IgA production (15)) but are not essential for controlling chronic bacterial infection in mouse lung.

Our study further provided insights on the roles of B and T cell subsets in the formation of bacteria-driven TLS in the lung. First, our data revealed that B cells, $CD4^+$ T cells and $CD8^+$ T cells are all required for the formation of germinal centers, which are the hallmark of TLS in which antigen-specific adaptive immune responses can be initiated (21, 22). Second, anti-CD20 mAb depletes B cells in TLS without affecting T cell aggregates, whereas combined treatment with anti-CD4/anti-CD8 mAbs reduced both the numbers of T cell and B cell aggregates. Mouse depleted exclusively in CD4+ T cells had comparable numbers of B cell aggregates that were nevertheless smaller. These data are somewhat different with findings by Eddens et al. who reported that depletion of $CD4^+$T cells with an anti-CD4 mAb abrogates the organization of B cell follicles and impairs the accumulation and proliferation of activated B cells (20). In the present *S. aureus* model, disorganization of the B cell follicles required depletion of both $CD4^+$ and $CD8^+$ T cells, whereas isolated depletion of only $CD4^+$ or $CD8^+$ T cells did not reduce the number of $CD20^+$ peribronchial lymphoid aggregates, indicating that both $CD4^+$ and $CD8^+$ T cells are involved in B cell recruitment and/or proliferation in this model. These data also suggest that CD8+ T cells are not involved in the recruitment of B cells but are important for the maturation of TLS marked by the appearance of GC. Our data on CD8+ T cell depletion also parallel the report by Curtis et al (23) that

showed that depletion of CD8+ T cells does not decrease the recruitment of immune cells. However, in the latter study, the impact of CD8+ T cell depletion on TLS was not documented. We further speculate that reduction in the size of peribronchial lymphoid aggregates in *S. aureus*-infected animals pretreated with anti-CD4 mAb is related to reduction in $CD4^+$ T follicular helper (Tfh) cells, which have been described to support B cell antigenic selection, survival and proliferation (24).

The present study has strengths and limitations. Our animal model is derived from the seminal model of Cash et al. (25) in which bacteria were embedded in agarose bead. This model mimics prolonged infection in CF airways where bacteria are often entrapped in mucus plugs in airway lumen (26, 27). In this model, peribronchial lymphoid neogenesis was limited to focal areas where infected agarose beads are present (6). Although the agarose bead model was developed with the aim of escaping the host immune environment in the lung (25, 28), Bragonzi et al. have shown that bacteria are found as macrocolonies inside and outside the beads in the airway lumen (29), an observation that was also found in our studies (Regard and Burgel, *personal communication*). Importantly, studies have shown that agarose bead-embedded bacteria proliferate within murine airways and that bacterial load can be decreased by treatment with antimicrobial agents (30, 31). In experiments aimed at assessing the impact of lymphocytes depletion, treatment of mice with anti-CD20 antibody effectively targeted $CD20^+$ B cells, which were undetectable in blood and lungs of treated animals for at least 21 days. Protocols used for targeting T cells were more complex to establish as they required repeated injection of anti-CD4 and anti-CD8 mAbs and did not eliminate $CD3^+/CD4^-/CD8^-$ T lymphocytes. However, these protocols made it possible to examine the individual and combined contribution of $CD4^+$ and $CD8^+$ T cells to lymphoid neogenesis.

Lymphoid follicles containing germinal centers are found in multiple chronic airway diseases, including severe asthma, severe COPD, and CF and non-CF bronchiectasis, but their roles remain incompletely

understood. The presence of TLS within the lungs of patients with COPD have been associated with disease progression (32) and lung B cells, as determined by gene expression profiling, showed consistent correlations with emphysema severity (33). Studies have reported the major role of B-cell activating factor (BAFF) in the development of TLS and alveolar destruction in response to cigarette smoke exposure in mice (34), findings that are highly relevant to patients with COPD (32). Further, uMT mice, which lack B-cells, had neither lymphoid follicle nor emphysema after exposure to cigarette smoke (35). In the latter study, authors also found that B cells are potent regulators of macrophage accumulation and macrophage-derived MMP12 production, contributing to emphysema development. Thus, the role of TLS in the development of emphysema is well established in animal models. Our experiments were designed to examine the role of TLS in infection control but additional studies would be necessary to examine the possible contribution of TLS to airway remodeling in the context of persistent bacterial infection. An unproven, yet testable, hypothesis would be that TLS may contribute to the development of bronchiectasis.

In conclusion, our study suggests that peribronchial TLS that develop during persistent airway infection triggered by agarose-bead embedded bacteria are not essential for controlling persistent bacterial infection in the lung. It further shows that lymphoid neogenesis is a highly coordinated event in which $CD20^+$ B lymphocytes, and $CD4^+$ and $CD8^+$ T lymphocytes are required for the formation of germinal centers where antigen-specific adaptive immune responses can be initiated via specific B cell selection and proliferation. Future studies should concentrate on the lifespan of TLS within the airways and their possible roles on promoting airway remodeling in the context of chronic bacterial infection.

Acknowledgment : We thank Genentech (San Francisco, CA, USA) for providing the anti-CD20 antibody that was used for B cell depletion.

Financial support : This work was funded by Vaincre la Mucoviscidose and La Fondation du Souffle/Fonds de Recherche en Santé Respiratoire and by Legs Pascal Bonnet. Funding sources were not involved in the study design; the collection, analysis and interpretation of the data; the writing of the report and the decision to submit the article for publication.

References

1. Burgel PR, Montani D, Danel C, Dusser DJ, Nadel JA. A morphometric study of mucins and small airway plugging in cystic fibrosis. Thorax. 2007;62(2):153-61.

2. Boucher RC. Muco-Obstructive Lung Diseases. N Engl J Med. 2019;380(20):1941-53.

3. Cantin AM, Hartl D, Konstan MW, Chmiel JF. Inflammation in cystic fibrosis lung disease: Pathogenesis and therapy. Journal of cystic fibrosis : official journal of the European Cystic Fibrosis Society. 2015;14(4):419-30.

4. Marteyn BS, Burgel PR, Meijer L, Witko-Sarsat V. Harnessing Neutrophil Survival Mechanisms during Chronic Infection by Pseudomonas aeruginosa: Novel Therapeutic Targets to Dampen Inflammation in Cystic Fibrosis. Frontiers in cellular and infection microbiology. 2017;7:243.

5. Chalmers JD, Hill AT. Mechanisms of immune dysfunction and bacterial persistence in non-cystic fibrosis bronchiectasis. Molecular immunology. 2013;55(1):27-34.

6. Frija-Masson J, Martin C, Regard L, Lothe MN, Touqui L, Durand A, et al. Bacteria-driven peribronchial lymphoid neogenesis in bronchiectasis and cystic fibrosis. Eur Respir J. 2017;49(4).

7. Lammertyn EJ, Vandermeulen E, Bellon H, Everaerts S, Verleden SE, Van Den Eynde K, et al. End-stage cystic fibrosis lung disease is characterised by a diverse inflammatory pattern: an immunohistochemical analysis. Respir Res. 2017;18(1):10.

8. Regard L, Martin C, Zemoura L, Geolier V, Sage E, Burgel PR. Peribronchial tertiary lymphoid structures persist after rituximab therapy in patients with cystic fibrosis. Journal of clinical pathology. 2018;71(8):752-3.

9. Polverino F, Lu B, Quintero JR, Vargas SO, Patel AS, Owen CA, et al. CFTR regulates B cell activation and lymphoid follicle development. Respir Res. 2019;20(1):133.

10. Whitwell F. A study of the pathology and pathogenesis of bronchiectasis. Thorax. 1952;7(3):213-39.

11. Teillaud JL, Regard L, Martin C, Siberil S, Burgel PR. Exploring the Role of Tertiary Lymphoid Structures Using a Mouse Model of Bacteria-Infected Lungs. Methods in molecular biology (Clifton, NJ). 2018;1845:223-39.

12. Hwang JY, Randall TD, Silva-Sanchez A. Inducible Bronchus-Associated Lymphoid Tissue: Taming Inflammation in the Lung. Frontiers in immunology. 2016;7:258.

13. Marin ND, Dunlap MD, Kaushal D, Khader SA. Friend or Foe: The Protective and Pathological Roles of Inducible Bronchus-Associated Lymphoid Tissue in Pulmonary Diseases. Journal of immunology (Baltimore, Md : 1950). 2019;202(9):2519-26.

14. Yadava K, Marsland BJ. Lymphoid follicles in chronic lung diseases. Thorax. 2013;68(6):597-8.

15. Ladjemi MZ, Martin C, Lecocq M, Detry B, Nana FA, Moulin C, et al. Increased IgA Expression in Lung Lymphoid Follicles in Severe Chronic Obstructive Pulmonary Disease. Am J Respir Crit Care Med. 2019;199(5):592-602.

16. Moyron-Quiroz JE, Rangel-Moreno J, Kusser KR, Hartson L, Sprague F, Goodrich S, et al. Role of inducible bronchus associated lymphoid tissue (iBALT) in respiratory immunity. Nat Med. 2004;10(9):927-34.

17. Tan HX, Esterbauer R, Vanderven HA, Juno JA, Kent SJ, Wheatley AK. Inducible Bronchus-Associated Lymphoid Tissues (iBALT) Serve as Sites of B Cell Selection and Maturation Following Influenza Infection in Mice. Frontiers in immunology. 2019;10:611.

18. Khader SA, Guglani L, Rangel-Moreno J, Gopal R, Junecko BA, Fountain JJ, et al. IL-23 is required for long-term control of Mycobacterium tuberculosis and B cell follicle formation in the infected lung. Journal of immunology (Baltimore, Md : 1950). 2011;187(10):5402-7.

19. Slight SR, Rangel-Moreno J, Gopal R, Lin Y, Fallert Junecko BA, Mehra S, et al. CXCR5(+) T helper cells mediate protective immunity against tuberculosis. The Journal of clinical investigation. 2013;123(2):712-26.

20. Eddens T, Elsegeiny W, Garcia-Hernadez ML, Castillo P, Trevejo-Nunez G, Serody K, et al. Pneumocystis-Driven Inducible Bronchus-Associated Lymphoid Tissue Formation Requires Th2 and Th17 Immunity. Cell reports. 2017;18(13):3078-90.

21. Pitzalis C, Jones GW, Bombardieri M, Jones SA. Ectopic lymphoid-like structures in infection, cancer and autoimmunity. Nature reviews Immunology. 2014;14(7):447-62.

22. Randall TD. Bronchus-associated lymphoid tissue (BALT) structure and function. Advances in immunology. 2010;107:187-241.

23. Curtis JL, Byrd PK, Warnock ML, Beck JM, Kaltreider HB. Pulmonary lymphocyte recruitment: depletion of CD8+ T cells does not impair the pulmonary immune response to intratracheal antigen. Am J Respir Cell Mol Biol. 1993;9(1):90-8.

24. Aloulou M, Fazilleau N. Regulation of B cell responses by distinct populations of CD4 T cells. Biomed J. 2019;42(4):243-51.

25. Cash HA, Woods DE, McCullough B, Johanson WG, Jr., Bass JA. A rat model of chronic respiratory infection with Pseudomonas aeruginosa. The American review of respiratory disease. 1979;119(3):453-9.

26. Baltimore RS, Christie CD, Smith GJ. Immunohistopathologic localization of Pseudomonas aeruginosa in lungs from patients with cystic fibrosis. Implications for the pathogenesis of progressive lung deterioration. The American review of respiratory disease. 1989;140(6):1650-61.

27. Mongodin E, Bajolet O, Hinnrasky J, Puchelle E, de Bentzmann S. Cell wall-associated protein A as a tool for immunolocalization of Staphylococcus aureus in infected human airway epithelium. The journal of histochemistry and cytochemistry : official journal of the Histochemistry Society. 2000;48(4):523-34.

28. Lorenz A, Pawar V, Haussler S, Weiss S. Insights into host-pathogen interactions from state-of-the-art animal models of respiratory Pseudomonas aeruginosa infections. FEBS letters. 2016;590(21):3941-59.

29. Bragonzi A, Paroni M, Nonis A, Cramer N, Montanari S, Rejman J, et al. Pseudomonas aeruginosa microevolution during cystic fibrosis lung infection establishes clones with adapted virulence. Am J Respir Crit Care Med. 2009;180(2):138-45.

30. Alhariri M, Omri A. Efficacy of liposomal bismuth-ethanedithiol-loaded tobramycin after intratracheal administration in rats with pulmonary Pseudomonas aeruginosa infection. Antimicrobial agents and chemotherapy. 2013;57(1):569-78.

31. Cigana C, Ranucci S, Rossi A, De Fino I, Melessike M, Bragonzi A. Antibiotic efficacy varies based on the infection model and treatment regimen for Pseudomonas aeruginosa. Eur Respir J. 2019;pii: 1802456.

32. Polverino F, Cosio BG, Pons J, Laucho-Contreras M, Tejera P, Iglesias A, et al. B Cell-Activating Factor. An Orchestrator of Lymphoid Follicles in Severe Chronic Obstructive Pulmonary Disease. Am J Respir Crit Care Med. 2015;192(6):695-705.

33. Faner R, Cruz T, Casserras T, López-Giraldo A, Noell G, Coca I, et al. Network Analysis of Lung Transcriptomics Reveals a Distinct B-Cell Signature in Emphysema. Am J Respir Crit Care Med. 2016;193(11):1242-53.

34. Seys LJ, Verhamme FM, Schinwald A, Hammad H, Cunoosamy DM, Bantsimba-Malanda C, et al. Role of B Cell-Activating Factor in Chronic Obstructive Pulmonary Disease. Am J Respir Crit Care Med. 2015;192(6):706-18.

35. John-Schuster G, Hager K, Conlon TM, Irmler M, Beckers J, Eickelberg O, et al. Cigarette smoke-induced iBALT mediates macrophage activation in a B cell-dependent manner in COPD. Am J Physiol Lung Cell Mol Physiol. 2014;307(9):L692-706.

Figure legends

Figure 1. Schematic representation of experiments assessing the effects of lymphocyte depletion on persistent *S. aureus* infection and lymphoid neogenesis in C57Bl/6 mice (results are shown in Figure 2 et Figure 3). Mice were pre-treated with anti-CD20 mAb (A), anti-CD4 and anti-CD8 mAbs (B), a combination of anti-CD20 and antiCD4/CD8 mAbs (C) prior to infection. For each depletion protocol, Control animals were injected with similar doses of isotype-matched control mAbs. Persistent infection was obtained by intratracheal instillation of agarose beads containing *S. aureus* (10^6 CFU per animal). Fourteen days after instillation, animals were euthanized and lungs were harvested for flow cytometry analysis, bacterial load assessment and immunohistochemical staining. A. *$CD20^+$ B cell depletion*: mice were injected intravenously with 250 μg of anti-CD20 mAb or Control mAb. B. *$CD4^+$ and $CD8^+$ T cell depletion*: to induce persistent $CD4^+$ and/or $CD8^+$ T cell depletion, mice received one intraperitoneal (*i.p.*) injection of anti-CD4 and/or anti-CD8 mAb (250 μg per injection) 4-5 days prior to infection and another *i.p*. injection 4-5 days after infection. C. Combined *$CD20^+$ B and $CD4^+$/$CD8^+$ T cell depletion*: $CD20^+$ B and $CD4^+$/$CD8^+$ T cell depletion protocols were combined to obtain prolonged $CD20^+$ B and $CD4^+$/$CD8^+$ T cell depletion. For each experiment, blood was sampled 24 hours before instillation and flow cytometry analysis was performed to confirm peripheral blood lymphocyte depletion.

Figure 2. Representative photomicrographs depicting the effects of $CD20^+$ B lymphocyte and/or $CD4^+$/$CD8^+$ T lymphocyte depletion on *S. aureus*-induced peribronchial lymphoid neogenesis.

Mice were pre-treated with control mAb or with anti-CD20 and/or anti-CD4/CD8 mAbs prior to infection. Persistent infection was obtained by intratracheal instillation of agarose beads containing *S. aureus* (10^6 CFU per animal). Beads (referred as "B" in the figure) are found in the airway lumen. Fourteen days after instillation, animals were euthanized and lungs were harvested for histological analysis**.** Sections were immunostained (brown color) with antibodies directed against B lymphocytes

($CD20^+$), follicular dendritic cells ($CD21^+$), T lymphocytes ($CD3^+$), and counterstained with hematoxylin. *Control mAbs*: in animal pretreated with Control mAb, 14-days infection with *S. aureus*- induced peribronchial tertiary lymphoid structures containing $CD20^+$ B cell areas with FDC and germinal centers, as well as $CD3^+$ T cell areas. *$CD20^+$ B cell depletion*: pretreatment with anti-CD20 mAb prevented B cell and FDC recruitment, and germinal center formation. T cells were unaffected. *$CD4^+$ and/or $CD8^+$ T cell depletion*: pretreatment with anti-CD4/CD8 mAbs strongly reduced $CD3^+$ T cell recruitment; $CD20^+$ B cells and FDCs were diminished, and germinal centers were absent. *$CD20^+$ B and $CD4^+$/$CD8^+$ T cell depletion*: pretreatment with anti-C20 and anti-CD4/CD8 mAbs prevented the recruitment of $CD20^+$ B cells and FDCs, and the formation of germinal centers. $CD3^+$ T cells were reduced. Symbols (*) identify areas represented in the inserts. . Original magnification, 100X;. Bar= 100 micrometres.

Figure 3. Quantitative morphometric analyses of B cell-, T cell- and FDC-containing lymphoid aggregates in the lungs of mice persistently infected with *S. aureus* and treated with anti-CD20, anti-CD4 plus CD8 mAbs or all three monoclonal antibodies.

Mice were pretreated with Control mAb or with anti-CD20 and/or anti-CD4/CD8 mAbs prior to infection. Persistent infection was obtained by intratracheal instillation of agarose beads containing *S. aureus* (10^6 CFU per animal). Fourteen days after instillation, animals were euthanized and lungs were harvested for histological analysis**.** Sections were immunostained with antibodies directed against B lymphocytes ($CD20^+$), follicular dendritic cells (FDCs, $CD21^+$) or T lymphocytes ($CD3^+$). Lymphoid aggregates were counted using morphometric analysis as described in the methods section. A. *$CD20^+$ B cell depletion*: pretreatment with anti-CD20 mAb significantly reduced the number of $CD20^+$ and FDC^+ lymphoid aggregates. $CD3^+$ T cell lymphoid aggregate number was unaffected. B. *$CD4^+$ and $CD8^+$ T cell depletion*: pretreatment with anti-CD4/CD8 mAbs significantly reduced the number of $CD3^+$ T cell-containing lymphoid aggregates; $CD20^+$ B cell- and FDC-containing lymphoid aggregate numbers were also

significantly reduced. C. *CD20$^+$ B- and CD4$^+$/CD8$^+$ T cell depletion*: pretreatment with anti-CD20 and anti-CD4/CD8 mAbs significantly reduced the number of CD20$^+$ and FDC$^+$-containing lymphoid aggregates, as well as the number of CD3$^+$ T cell$^+$ lymphoid aggregates. Each symbol represents data obtained from one animal. Horizontal bars correspond to median values. The Mann-Whitney test was used to compare depleted groups to Controls. *: *P*<0.05, **: *P*<0.01, ****: *P*<0.0001 compared to controls.

Figure 4. **Quantitative morphometric analyses of the effects of isolated vs. combined CD4$^+$ and CD8$^+$ T cell depletion on lymphoid neogenesis in the lungs of C57Bl/6 mice persistently infected with *S. aureus***.

Mice were treated with Control mAbs or with anti-CD4 and/or anti-CD8 mAbs prior to intratracheal instillation with *S. aureus*-containing beads. Animals were euthanized 14 days after instillation and lung were harvested for histological analyses. Sections were immunostained with antibodies to B lymphocytes (CD20$^+$), follicular dendritic cells (FDCs, CD21$^+$), germinal centers (proliferating cell nuclear antigen, PCNA$^+$), T lymphocytes (CD3$^+$), or high endothelial venules (peripheral node adressin, PNAd$^+$). Lymphoid aggregates were counted using morphometric analysis as described in Methods. Combined CD4$^+$/CD8$^+$ T cell depletion induced a significant decrease in number (A) and size (F) of peribronchial CD20$^+$ lymphoid aggregates, and reduced FDC recruitment, and HEV and germinal center formation. Pretreatment with anti-CD4 or anti-CD8 mAbs did not reduce the number of CD20$^+$ peribronchial lymphoid aggregates, the recruitment of FDC and the number of HEVs but prevented germinal center formation. However, injection of anti-CD4 mAb reduced the size of CD20$^+$ peribronchial lymphoid aggregates. Each symbol represents data obtained from one animal. Horizontal bars correspond to the median. Vertical bars in Figure 4F represent means and error bars represent standard deviations. The Kruskall-Wallis test corrected with Dunn's test was used to compare each depleted group to the Controls *: *P*<0.05, ***: *P*<0.001, ****: *P*<0.0001 compared to Controls.

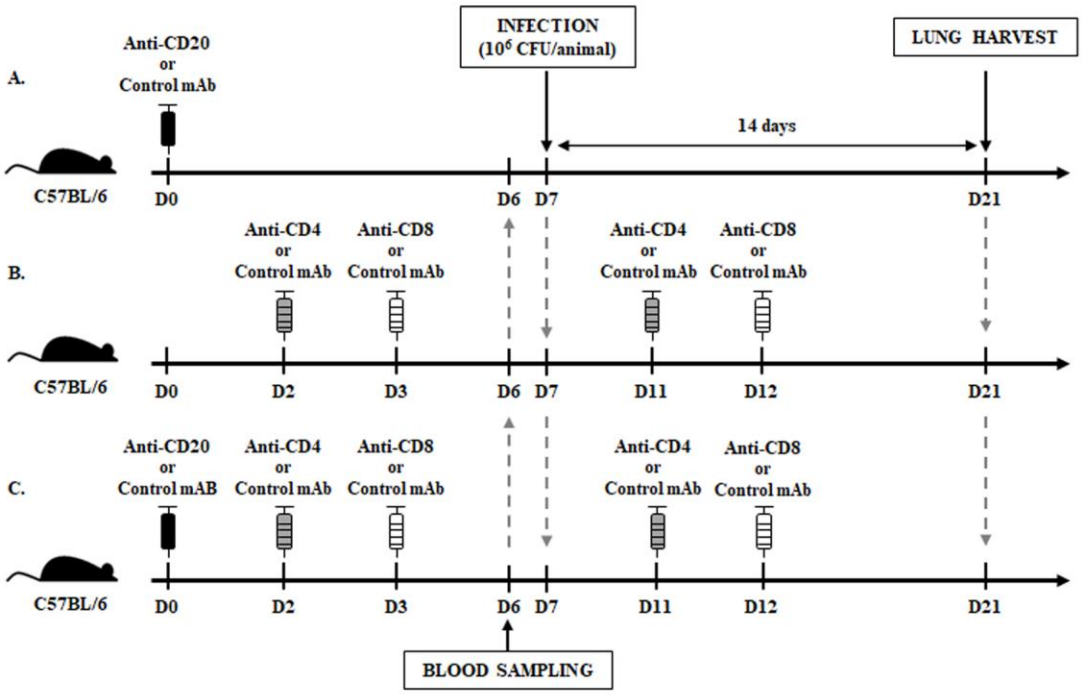
A.
Anti-CD20
or
Control mAb
INFECTION
(10^6 CFU/animal)
LUNG HARVEST
14 days
C57BL/6
D0
D6
D7
D21
B.
Anti-CD4
or
Control mAb
Anti-CD8
or
Control mAb
Anti-CD4
or
Control mAb
Anti-CD8
or
Control mAb
C57BL/6
D0
D2
D3
D6
D7
D11
D12
D21
C.
Anti-CD20
or
Control mAB
Anti-CD4
or
Control mAb
Anti-CD8
or
Control mAb
Anti-CD4
or
Control mAb
Anti-CD8
or
Control mAb
C57BL/6
D0
D2
D3
D6
D7
D11
D12
D21
BLOOD SAMPLING

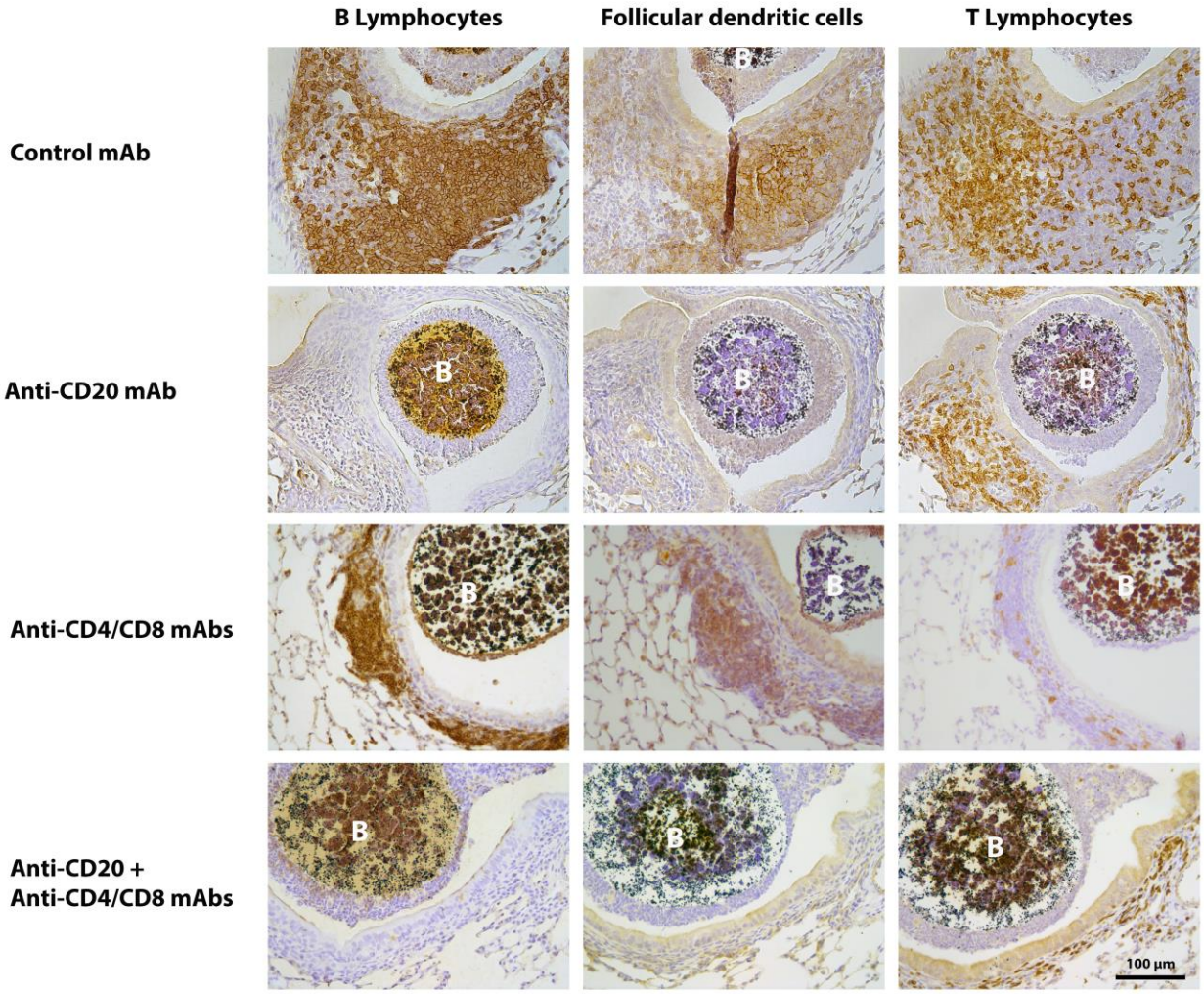
B Lymphocytes
Follicular dendritic cells
T Lymphocytes
Control mAb
Anti-CD20 mAb
Anti-CD4/CD8 mAbs
Anti-CD20 +
Anti-CD4/CD8 mAbs
B
100 µm

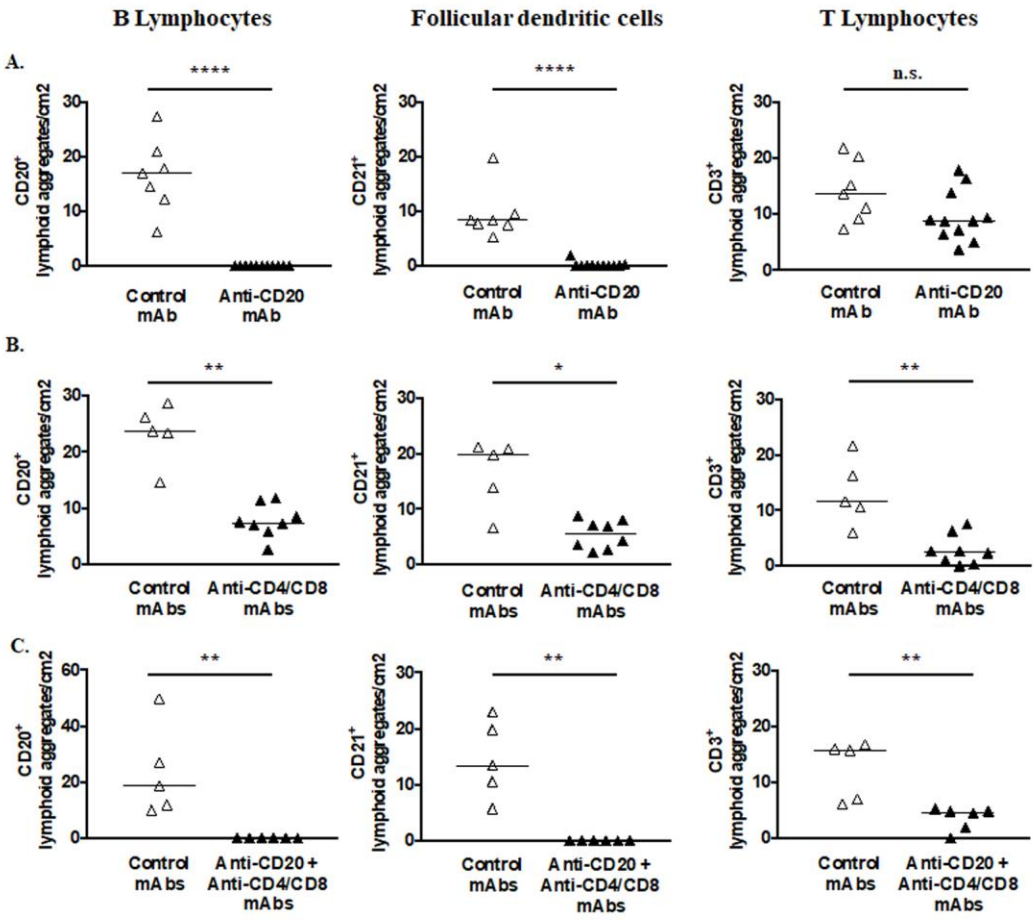
B Lymphocytes
Follicular dendritic cells
T Lymphocytes
A.
B.
C.
CD20+ lymphoid aggregates/cm2
CD21+ lymphoid aggregates/cm2
CD3+ lymphoid aggregates/cm2
****
n.s.
**
*
Control mAb
Anti-CD20 mAb
Control mAbs
Anti-CD4/CD8 mAbs
Anti-CD20 + Anti-CD4/CD8 mAbs

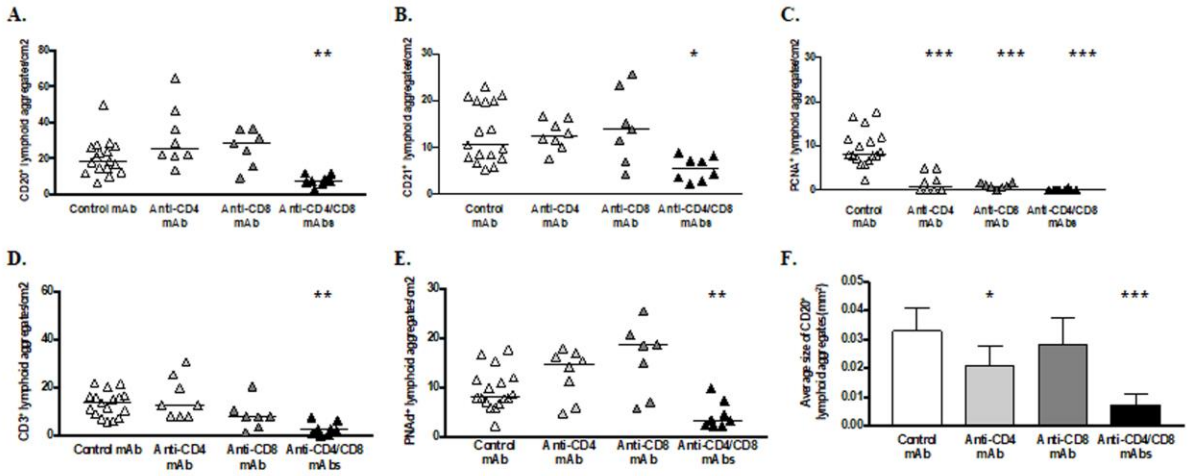
A.
B.
C.
D.
E.
F.
CD20+ lymphoid aggregates/cm2
CD21+ lymphoid aggregates/cm2
PCNA+ lymphoid aggregates/cm2
CD3+ lymphoid aggregates/cm2
PNAd+ lymphoid aggregates/cm2
Average size of CD20+ lymphoid aggregates(mm2)
Control mAb
Anti-CD4 mAb
Anti-CD8 mAb
Anti-CD4/CD8 mAbs
*
**
***

Table S1. Primary antibodies used for immunohistochemical staining in mouse lung sections

Antigen	Source	Manufacturer	Reference	Dilution	Unmasking
Mouse CD20	Goat polyclonal	Santa Cruz	Sc7735	1:100	Citrate microwave
Mouse CD3	Rabbit monoclonal	ThermoFisher	RM-9207-S	1:50	Citrate microwave
Mouse CD21	Rabbit monoclonal	Abcam	Ab 75985	1:200	Citrate microwave
Mouse PNAd	Rat monoclonal	BD Pharmingen	553863	1:50	Citrate microwave
Mouse PCNA	Rabbit polyclonal	Calbiochem	PC474	1:200	Protease

PNAd: peripheral nod adressin; PCNA: proliferating cell nuclear antigen

Table S2. Antibody panels used in flow cytometry analysis.

Fluorochrome	Antigen (Antibody clone)
FITC	B220 (RA3-6B2)*
BV450	CD19 (1D3)*
PE-TexasRed	CD4 (MCD0417)£
PE-Cy7	CD45 (30-F11)*
APC	CD8 (53-6.7)*
AF700	CD3 (500A2)*
Amcyan	Viability marker (Live/dead cell dye)£

Conjugated antibodies or fluorescent dyes were purchased from *BD Bioscience, £ThermoFisher Scientific.

Figure S1. Treatment with anti-CD20 and/or anti-CD4/CD8 mAbs induces depletion in lung of B and /or T lymphocytes for at least 21 days.

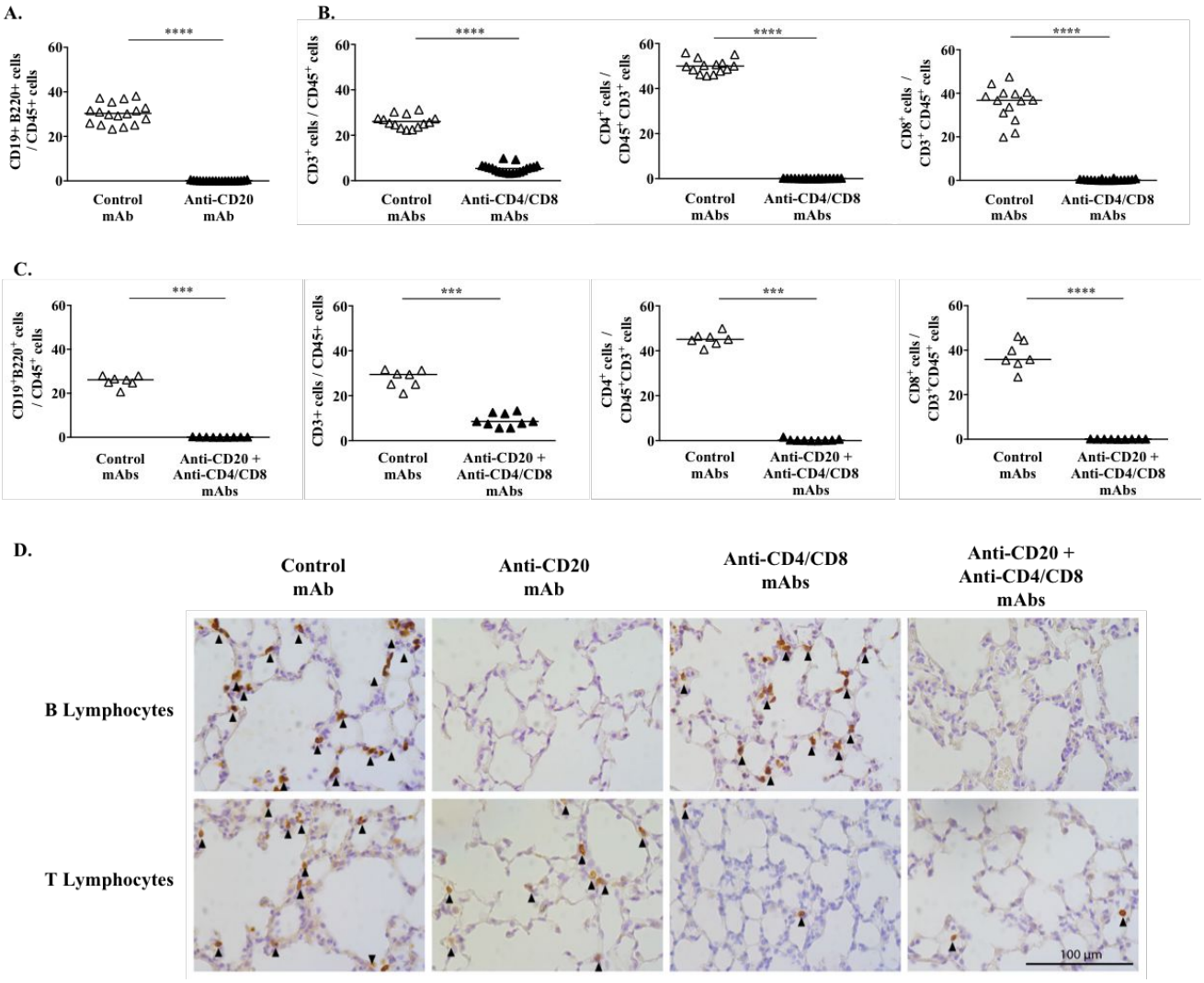

Mice were injected with anti-CD20 and/or anti-CD4/CD8 mAbs, or control mAbs and followed for 21 days (no infection). At 21 days after treatment with mAbs, lungs were harvested for flow cytometry (A, B, C) and histological analysis (D). A. Quantification of B cells obtained by flow cytometry analysis in the lungs of mice treated with control or anti-CD20 mAb. B. Quantification of T cell subsets (CD3+CD45+ [left panel], CD4+CD3+CD45+ [middle panel] and CD8+CD3+CD45+ [right panel]) obtained by flow cytometry analysis in the lungs of mice treated with control mAbs or anti-CD4/CD8 mAbs. C.

Quantification of B cells and T cell subsets in the lungs of mice treated with control mAbs or with both anti-CD20 and anti-CD4/CD8 mAbs. Each symbol represents data obtained from one animal (open symbol for Controls and solid symbols for depleted mice). Horizontal bars represent medians. The Mann-Withney test was used to compare depleted mice to Controls (Panel A, B and C). ****$p < 0.0001$ and ***$p<0.001$ compared to controls. D. Representative photomicrographs of immunostaining for B lymphocytes (CD20+, upper panel) or T lymphocytes (CD3+, lower panel) in the lungs of mice sacrificed 21 days after treatment with control mAb or anti-CD20 mAb, or anti-CD4/CD8 mAbs, or anti-CD20 and anti-CD4/CD8 mAbs. Positive staining appears in brown (arrowheads); sections were counterstained with hematoxylin. Original magnification, 400X.

Figure S2. Effects of anti-CD20 and/or anti-CD4/CD8 mAbs-induced depletion on lung bacterial load in mice persistently infected with *S. aureus*.

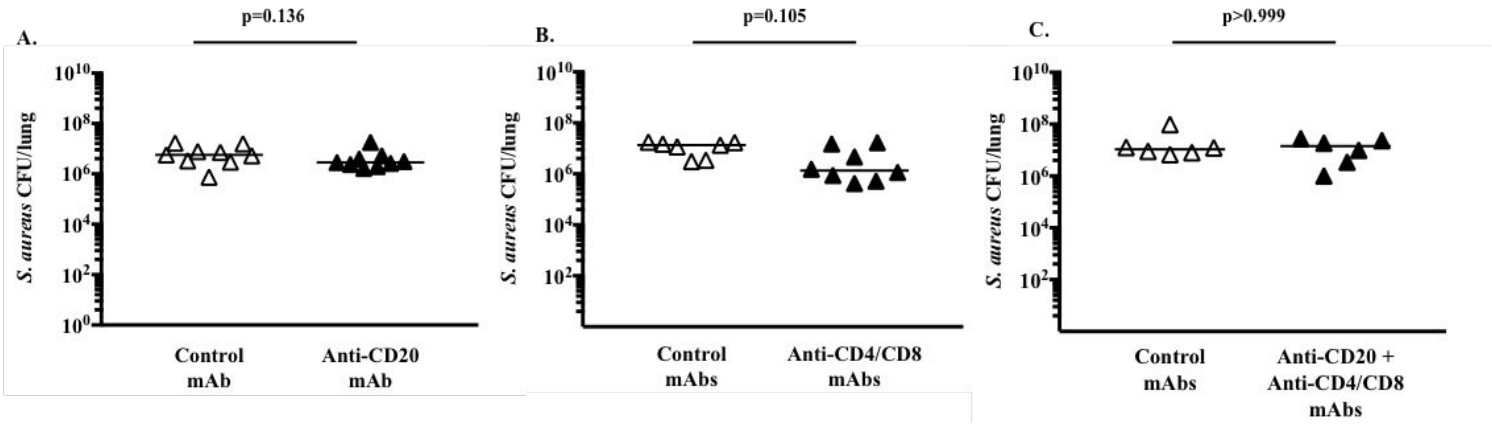

Mice were pre-treated with anti-CD20 mAb (A), anti-CD4 and anti-CD8 mAbs (B), or a combination of anti-CD20 and anti-CD4/CD8 mAbs (C) or with Control mAb prior to infection. Persistent infection was obtained by intratracheal instillation of agarose beads containing S. aureus (10^6 CFU per animal). Fourteen days after instillation, animals were sacrificed and lungs were harvested, homogenized and cultured for bacterial load assessment. Pretreatment with anti-CD20, anti-CD4/CD8 or a combination of anti-CD20 and anti-CD4/CD8 mAbs had no effect on lung bacterial load compared to control group. Each symbol represents data obtained from one animal. Horizontal bars correspond to medians. The Mann-Whitney test was used to compare depleted mice to Controls (Panel A, B and C).

Figure S3. Representative photomicrographs of *S. aureus*-induced peribronchial lymphoid neogenesis in mice treated with control mAb.

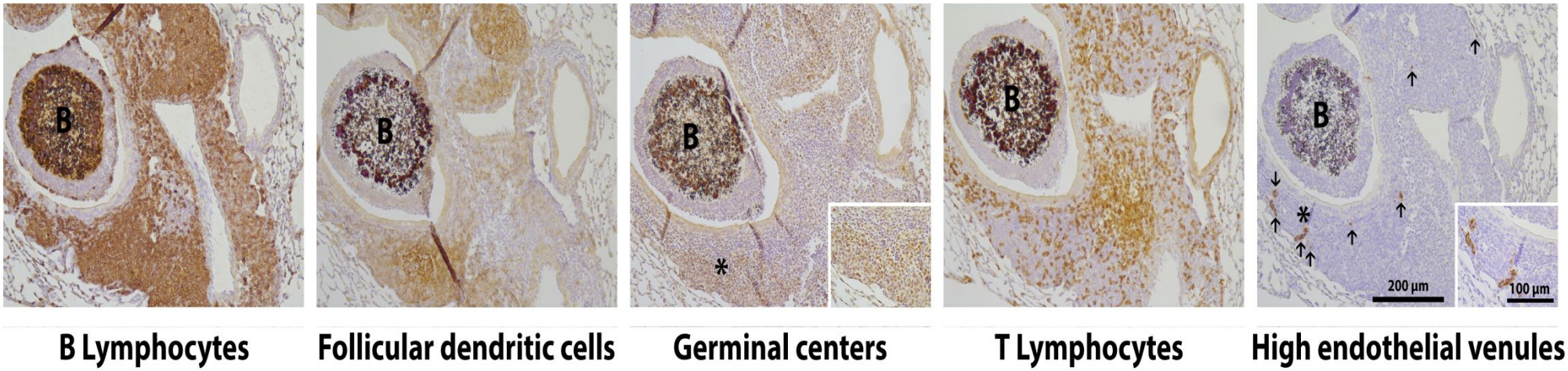

Mice were pre-treated with control mAb. Persistent infection was obtained by intratracheal instillation of agarose beads containing *S. aureus* (10^6 CFU per animal). Beads (referred as "B" in the figure) are found in the lumen of the mice bronchi. Fourteen days after instillation, animals were euthanized and lungs were harvested for histological analysis**.** Sections were immunostained (brown color) with antibodies directed against B lymphocytes ($CD20^+$), follicular dendritic cells ($CD21^+$), germinal centers (proliferating cell nuclear antigen, $PCNA^+$), T lymphocytes ($CD3^+$), or high endothelial venules (HEVs, peripheral node adressin, $PNAd^+$), and counterstained with hematoxylin. Peribronchial lymphoid aggregates were found around bead-containing bronchi; these aggregates contained B-cell areas ($CD20^+$) with follicular dendritic cells ($CD21^+$) and germinal centers ($PCNA^+$) and were surrounded by T cell aggregates ($CD3^+$) containing high endothelial venules ($PNAd^+$) and were consistent

with tertiary lymphoid structures. Symbols (*) identify areas represented in the inserts. Arrows identify HEVs. Original magnification, 100X; inserts, 400X. Bar= 200 micrometers; insert bar = 100 micrometres.

Figure S4. Representative photomicrographs of germinal centers and HEV in the lungs of mice persistently infected with *S. aureus* and treated with anti-CD20, anti-CD4 plus CD8 mAbs or all three monoclonal antibodies.

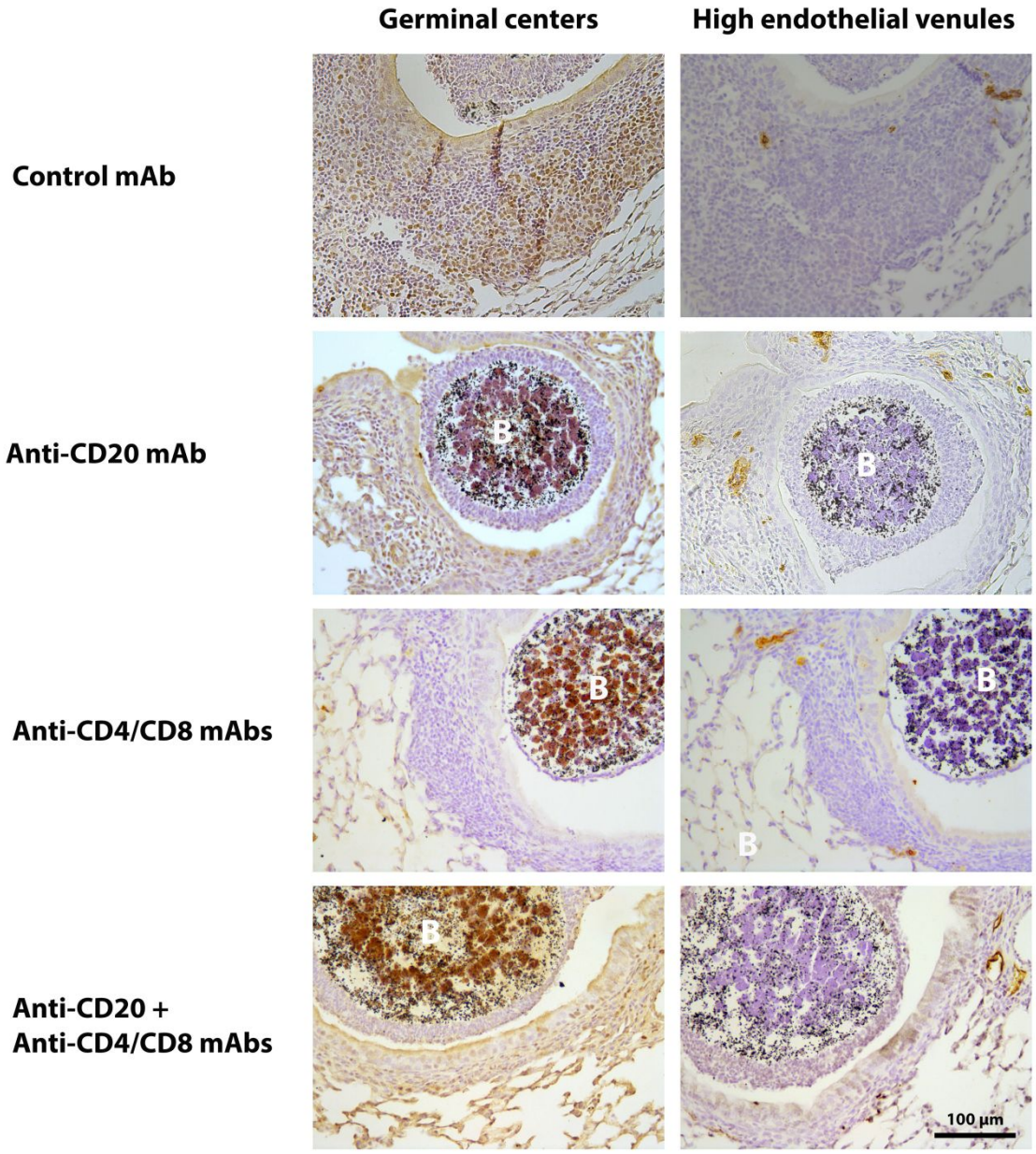

Mice were pre-treated with control mAb or with anti-CD20 and/or anti-CD4/CD8 mAbs prior to infection. Persistent infection was obtained by intratracheal instillation of agarose beads containing *S. aureus* (10^6 CFU per animal). Beads (referred as "B" in the figure) are found in the lumen of the mice bronchi. Fourteen days after instillation, animals were euthanized and lungs were harvested for histological analysis**.** Sections were immunostained (brown color) with antibodies directed against germinal centers (proliferating cell nuclear antigen, $PCNA^+$)

or high endothelial venules (HEVs, peripheral node adressin, $PNAd^+$), and counterstained with hematoxylin. *Control mAbs*: in animal pretreated with Control mAb, 14-days infection with *S. aureus*- induced peribronchial tertiary lymphoid structures containing germinal centers, as well as HEV. *$CD20^+$ B cell depletion*: pretreatment with anti-CD20 mAb prevented germinal center formation. HEV recruitment was unaffected. *$CD4^+$ and/or $CD8^+$ T cell depletion*: pretreatment with anti-CD4/CD8 mAbs reduced HEVs formation and germinal centers were absent. *$CD20^+$ B and $CD4^+$/$CD8^+$ T cell depletion*: pretreatment with anti-C20 and anti-CD4/CD8 mAbs prevented the formation of germinal centers. HEVs were reduced. Arrows identify HEVs. Original magnification, 100X. Bar= 100 micrometers.

Figure S5. Quantitative morphometric analyses of germinal center- and HEV-containing lymphoid aggregates in the lungs of mice persistently infected with *S. aureus* and treated with anti-CD20, anti-CD4 plus CD8 mAbs or all three monoclonal antibodies.

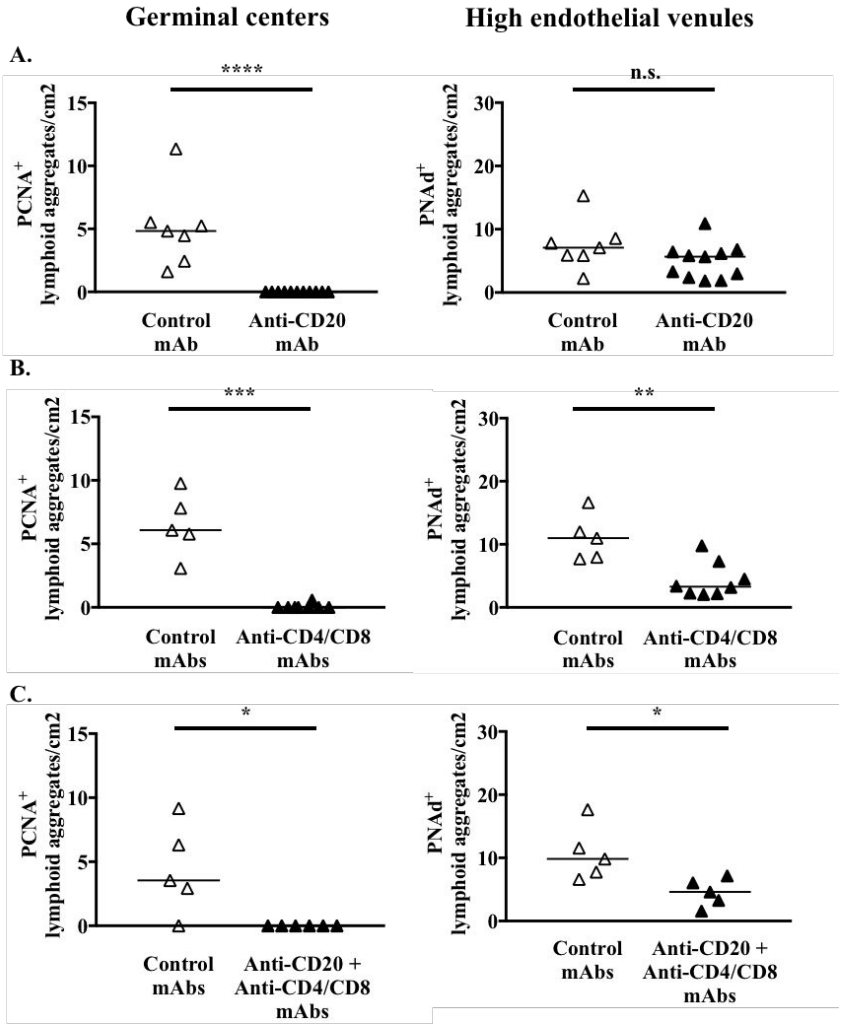

Mice were pretreated with Control mAb or with anti-CD20 and/or anti-CD4/CD8 mAbs prior to infection. Persistent infection was obtained by intratracheal instillation of agarose beads containing *S. aureus* (10^6 CFU per animal). Fourteen days after instillation, animals were euthanized and lungs were harvested for histological analysis**.** Sections were immunostained with antibodies directed against germinal center (proliferating cell nuclear antigen, $PCNA^+$), or high endothelial venules (peripheral node adressin, $PNAd^+$). Lymphoid aggregates were counted using morphometric analysis as described in the methods section. A. *$CD20^+$ B cell*

depletion: pretreatment with anti-CD20 mAb significantly reduced the number of germinal center-containing lymphoid aggregates. HEV^+ lymphoid aggregate number was unaffected. B. *$CD4^+$ and $CD8^+$ T cell depletion*: pretreatment with anti-CD4/CD8 mAbs significantly reduced the number of germinal center-containing lymphoid aggregate; HEV-containing lymphoid aggregates number was also significantly reduced. C. *$CD20^+$ B- and $CD4^+$/$CD8^+$ T cell depletion*: pretreatment with anti-CD20 and anti-CD4/CD8 mAbs significantly reduced the number of germinal center-containing lymphoid aggregates, as well as the number of HEV^+ lymphoid aggregates. Each symbol represents data obtained from one animal. Horizontal bars correspond to median values. The Mann-Whitney test was used to compare depleted groups to Controls. *: $P<0.05$, **: $P<0.01$, ***: $P<0.001$, ****: $P<0.0001$ compared to controls.